Low Temperature Heat Capacity and Thermodynamic Functions of Ceria-Stabilized Zirconia $Ce_{0.124}Zr_{0.876}O_2$

Takeo Tojo,* Hitoshi Kawaji, and Tooru Atake

Materials and Structures Laboratory, Tokyo Institute of Technology, 4259 Nagatsuta-cho, Midori-ku, Yokohama 226-8503, Japan

Toshiyuki Mori

National Institute for Materials Science, 1-2-1 Sengen, Tsukuba 305-0047, Japan

Hiroshi Yamamura

Department of Applied Chemistry, Faculty of Engineering, Kanagawa University, 3-27-1 Rokkakubashi, Kanagawa-ku, Yokohama 221-8686, Japan

The heat capacity of $Ce_{0.124}Zr_{0.876}O_2$ was measured by adiabatic calorimetry between 13 and 300 K. The smoothed values of the molar heat capacity were obtained from the measured data with a least-squares method. The enthalpy, entropy, and Gibbs energy of $Ce_{0.124}Zr_{0.876}O_2$ were also calculated from the smoothed values and tabulated at selected temperatures from (13 to 300) K. The heat capacity, enthalpy, and entropy at $T = 298.15$ K were 57.34 $J{\cdot}K^{-1}$ mol^{-1}, 9.169 $kJ{\cdot}mol^{-1}$, and 53.74 $J{\cdot}K^{-1}{\cdot}mol^{-1}$, respectively. Neutron inelastic scattering experiments were also carried out to investigate the phonon density of states. The mechanism of phonon-mode softening in $Ce_{0.124}Zr_{0.876}O_2$ was discussed.

Introduction

Stabilized zirconia is one of the most promising materials for use as solid electrolytes in oxide fuel cells and as oxygen sensors. The properties relating to such applications depend strongly on both the average crystal structure and the local defect structure. Pure zirconia has three polymorphs below the melting point under ambient pressure. The highest-temperature phase has a face-centered cubic fluorite-type structure,[1] and the crystal undergoes structural phase transitions from cubic to tetragonal at 2640 K and from tetragonal to monoclinic at 1440 K. Both tetragonal and monoclinic phases have a distorted fluorite structure.[2,3] The stable phase of pure zirconia at room temperature is monoclinic. A zirconium ion in the cubic and tetragonal phases is coordinated by eight oxygen ions. However, the local structure of the monoclinic phase is different from that of the high-temperature phases, and the zirconium ion is coordinated by seven oxygen ions. It is well-known that the higher-temperature phases can be stabilized to even below room temperature by adding di- or trivalent oxides such as CaO, Y_2O_3, and so on. By such doping, a large number of oxygen vacancies are formed in the anion sublattice, as required by electrical neutrality. The vacancies are reported to be responsible for the high ionic conductivity of stabilized zirconia.[4,5] The electrical conductivity increases with increasing vacancies at low concentration. However, electrical conductivity shows a maximum at about several percent of dopant concentration and then decreases with further doping. The conductivity maximum is located near the tetragonal + cubic/cubic two-phase boundary in the equilibrium phase diagram of stabilized zirconia. Several models for the concentration dependence in the electrical conductivity have been proposed: defect association,[6] vacancy−vacancy interaction,[7] microdomain formation,[8] and so on. However, the mechanism has not yet been clarified.

The defect structure of stabilized zirconia is very complicated. In yttria-stabilized zirconia,[9−12] the dopants and vacancies are not distributed randomly on the lattice site. The EXAFS study[13,14] suggested that the oxygen vacancies are sited in the first neighbors to the Zr ions. The defects cause a significant lattice relaxation. Oxygen ions and cations in the vicinity are displaced from their ideal positions in the fluorite structure. It is well-known that the defects and local structures in a crystal influence the lattice vibrations and thus the heat capacity.

Recently, we measured the heat capacity of yttria-stabilized zirconia with several dopant concentrations and found an excess heat capacity extending from liquid helium temperature to room temperature.[15−17] The excess heat capacity is attributed to an increase in the number of low-frequency phonons, which is ascribed to the formation of oxygen defects and/or the stabilization of the high-temperature phase structure. Results from the analysis of the concentration dependence of the excess heat capacity indicate that the difference in the local atomic arrangements between monoclinic and high-temperature phase structure, that is, the difference in the oxygen coordination number of zirconium ions between the two phases, could lead to the large number of low-frequency phonons in stabilized zirconia.[17] However, the effects of the formation of oxygen defects cannot be excluded completely.

Doping of ceria also stabilizes the high-temperature phases of zirconia.[19,20] In ceria-stabilized zirconia, however, no oxygen defect is formed because cerium ions exist as

* To whom correspondence should be addressed. Telephone: (81)-45-924-5343. Fax: (81)-45-924-5339. E-mail: ttojo@msl.titech.ac.jp.

10.1021/je034052q CCC: $25.00
Published on Web 10/23/2003

tetravalent ions and substitute the Zr^{4+} ions with the same valence. Thus, the effect of the stabilization of the high-temperature phase on the lattice vibrations of zirconia can be studied in this solid solution system. In the present study, precise heat capacity measurements on $Ce_{0.124}Zr_{0.876}O_2$ were made by adiabatic calorimetry between (13 and 300) K. From the results, the thermodynamic functions, enthalpy, entropy, and Gibbs energy, were derived. Neutron inelastic scattering experiments were also performed to determine the phonon density of states. The physical mechanism of softening of phonon modes, which should give the excess heat capacity at low temperatures, is discussed in comparison with the case of yttria-stabilized zirconia.

Experimental Section

The sample was synthesized by a hydrolysis method from the mixture of $ZrOCl_2 \cdot 8H_2O$ (Tosoh Co. Ltd., Japan) solution and $CeCl_3$ (commercial grade) solution. The hydrolysis products were spray-dried and treated in a steam flow for dechlorination. The powders obtained were uniaxially pressed into plates under a pressure of 50 MPa and then isostatically cold-pressed at 200 MPa. The pellets were sintered at 1773 K in an oxygen atmosphere for 4 h. The obtained sample was a mixture of the monoclinic and tetragonal phases, as reported previously.[20] The mass fraction was estimated to be 70% monoclinic and 30% tetragonal by X-ray diffractometry. The sample is considered to be homogeneous in composition, since the monoclinic phase forms in the tetragonal phase through the diffusionless phase transition during cooling.[20] Such two-phase zirconia is termed as a partially stabilized zirconia. The compositon of the sample was determined to be $Ce_{0.124}Zr_{0.876}O_2$ by inductively coupled plasma (ICP) spectrometry.

For the heat capacity measurements, a sintered sample with the mass 15.553 g (0.120 28 mol) was loaded into the calorimeter vessel (gold-plated copper), which was evacuated and then sealed after adding a small amount of helium (5 kPa at room temperature) for the purpose of thermal uniformity within the calorimeter vessel. The heat capacity measurements were carried out using a homemade adiabatic calorimeter between (13 and 300) K. The temperature was measured with a platinum resistance thermometer (Tinsley, 5187L) calibrated at NPL (U.K.) on the basis of the ITS-90 scale. The adiabatic control system gave the temperature stability of the calorimeter vessel within 0.01 $mK \cdot min^{-1}$. The performance of the calorimeter was confirmed by measuring the standard reference material SRM 720 (synthetic sapphire) provided by NIST (U.S.A), which gave the accuracy of the heat capacity value of ±0.1% at 100 K. The precision of the data was better than ±0.05%. The heat capacity of the sample was obtained by subtracting that of the calorimeter vessel from the total heat capacity. The details of the method of the measurements were described elsewhere.[21,22]

The neutron inelastic scattering measurements were carried out using the inverted geometry time-of-flight spectrometer LAM-D installed at the pulsed neutron source in the KENS facility at KEK in Japan.[23] About 20 g of the same sample as used for calorimetry was put on an aluminum cylinder, and the experiments were performed at 17 K.

Results and Discussion

The heat capacity of $Ce_{0.124}Zr_{0.876}O_2$ was measured between (13 and 300) K. The temperature increment of each measurement was about 2 K. After each heat input, thermal equilibrium of the whole calorimeter vessel including the sample was attained in a few minutes below 20 K and about 10 min above 100 K. No anomalous relaxation nor hysteresis phenomenon was observed during the experiments. The molar heat capacity without curvature corrections is plotted in Figure 1 together with that of ZrO_2[16] and CeO_2,[24] and the numerical data are given in Table 1. The plots of $C_{p,m}T^{-3}$ against T are shown as the inset in Figure 1. The smoothed heat capacity curve was obtained from the primary data by a method of least-squares fitting; the heat capacity data were divided into six temperature regions, and each region was fitted by a polynomial expression up to the seventh degree. We made two sets of such fittings, which were divided by different temperatures, and they were averaged to obtain the smoothed values, so that the somewhat large fitting errors near the border were reduced. The heat capacity below 13 K was estimated by a graphical smooth extrapolation. The thermodynamic functions calculated from the smoothed heat capacity values at rounded temperatures are given in Table 2.

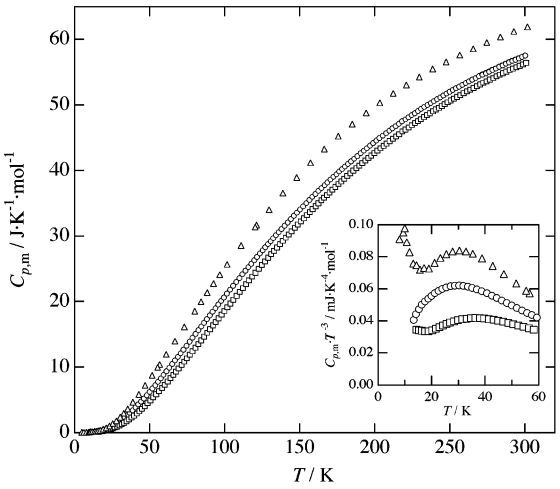

Figure 1. Measured molar heat capacity of $Ce_{0.124}Zr_{0.876}O_2$, together with those of ZrO_2 (ref 17) and CeO_2:[24] ○, $Ce_{0.124}Zr_{0.876}O_2$; □, ZrO_2; △, CeO_2. The inset shows the low-temperature data of $C_{p,m}T^{-3}$ against T.

In Figure 1, the heat capacity values of $Ce_{0.124}Zr_{0.876}O_2$ are between those of ZrO_2 and of CeO_2. Thus, we examined the additive property of the heat capacity. Since both the structures of zirconia and ceria are isostructural fluorite-type, a simple additivity rule may be applied as follows:

$$C_{p,m}(\text{calc}) = 0.124C_{p,m}(CeO_2) + 0.876C_{p,m}(ZrO_2) \quad (1)$$

where $C_{p,m}(CeO_2)$ and $C_{p,m}(ZrO_2)$ are the heat capacities of pure ceria and pure zirconia, respectively. The deviation of the measured heat capacity from the calculated heat capacity $\{\Delta C_{p,m} = C_{p,m} - C_{p,m}(\text{calc})\}$ is given in Figure 2, where those of yttria-stabilized zirconia calculated in the same manner are also plotted. Apparently the measured heat capacity of $Ce_{0.124}Zr_{0.876}O_2$ is larger than that obtained from the simple additivity rule of ZrO_2 and CeO_2. The excess heat capacity of $Ce_{0.124}Zr_{0.876}O_2$ is extended to a wide temperature range, and the shape is very similar to a Schottky anomaly. Similar excess heat capacity results have been observed in yttria-stabilized zirconia.[16,17] The temperature of the maximum excess heat capacity T_{max} of $Ce_{0.124}Zr_{0.876}O_2$ is about 88 K, which is somewhat higher than that of yttria-stabilized zirconia (77 K). The Schottky-type heat capacity of a two-level system can be described

Table 1. Measured Molar Heat Capacity $C_{p,m}$ of $Ce_{0.124}Zr_{0.876}O_2$

T	$C_{p,m}$	T	$C_{p,m}$	T	$C_{p,m}$
K	J·K^{-1}·mol^{-1}	K	J·K^{-1}·mol^{-1}	K	J·K^{-1}·mol^{-1}
			Series 1		
14.135	0.1243	99.524	20.606	196.85	43.799
15.208	0.1661	101.48	21.195	198.91	44.180
16.337	0.2182	103.57	21.789	201.02	44.573
17.521	0.2799	105.70	22.384	203.17	44.958
18.728	0.3529	107.80	22.996	205.33	45.320
19.966	0.4414	109.86	23.569	207.50	45.682
21.235	0.5468	111.88	24.153	209.66	46.073
22.569	0.6742	113.88	24.690	211.82	46.433
23.989	0.8271	115.84	25.244	213.96	46.763
25.505	1.0103	117.78	25.764	216.09	47.115
27.066	1.2211	119.69	26.286	218.21	47.502
28.656	1.4573	121.58	26.791	220.32	47.790
30.267	1.7184	123.45	27.325	222.42	48.131
31.890	2.0027	125.29	27.788	224.52	48.438
33.511	2.3058	127.12	28.276	226.60	48.735
35.146	2.6292	128.92	28.746	228.67	49.074
36.901	2.9954	130.70	29.212	230.79	49.390
38.751	3.4004	132.47	29.668	232.95	49.704
40.669	3.8459	134.22	30.124	235.10	50.002
42.549	4.2909	136.02	30.582	237.25	50.286
44.338	4.7310	137.94	31.066	239.38	50.597
46.182	5.1976	139.96	31.580	241.51	50.886
48.096	5.6942	142.03	32.080	243.63	51.175
49.976	6.1938	144.08	32.603	245.73	51.440
51.868	6.7035	146.11	33.100	247.83	51.729
53.780	7.2281	148.13	33.564	249.93	52.014
55.640	7.7450	150.16	34.055	252.01	52.289
57.476	8.2658	152.25	34.532	254.09	52.541
59.314	8.7872	154.34	35.038	256.22	52.786
61.219	9.3381	156.41	35.511	258.39	53.080
63.179	9.9019	158.47	35.980	260.58	53.349
65.102	10.464	160.51	36.430	262.79	53.604
66.964	11.009	162.53	36.896	265.00	53.876
68.806	11.546	164.54	37.335	267.19	54.107
70.666	12.095	166.53	37.762	269.38	54.383
72.551	12.652	168.51	38.192	271.56	54.642
74.550	13.244	170.48	38.609	273.74	54.872
76.623	13.861	172.43	39.037	275.94	55.080
78.650	14.465	174.37	39.432	278.15	55.352
80.616	15.047	176.29	39.835	280.36	55.556
82.546	15.619	178.21	40.212	282.57	55.803
84.444	16.181	180.15	40.597	284.77	56.043
86.296	16.737	182.18	41.003	286.96	56.276
88.193	17.300	184.23	41.388	289.14	56.491
90.136	17.871	186.33	41.807	291.31	56.725
92.036	18.428	188.46	42.205	293.48	56.917
93.913	18.977	190.57	42.628	295.65	57.107
95.773	19.520	192.68	43.019	297.81	57.305
97.636	20.062	194.77	43.407	299.96	57.521
			Series 2		
271.80	54.598	282.88	55.796	293.79	56.878
274.03	54.827	285.08	56.024	295.95	57.124
276.25	55.051	287.26	56.267	298.11	57.324
278.47	55.324	289.45	56.483	300.26	57.528
280.68	55.568	291.62	56.698		

as a difference of two Einstein-type heat capacities with frequencies ν and 2ν as[17]

$$C_{Sch}(h\nu,T) = C_{Ein}(h\nu,T) - C_{Ein}(2h\nu,T) \qquad (2)$$

where h is Plank's constant. The right-hand side of the equation means that the vibration modes at $2h\nu$ change its vibrational frequency into $h\nu$, that is, the softening of the phonon mode. It is well-known that the maximum temperature T_{max} in the Schottky-type heat capacity curve is represented as $k_B T_{max}/h\nu = 0.42$. Thus, the softened frequency ν is estimated to be 4.4 THz ($h\nu = 18$ meV) from the excess heat capacity of $Ce_{0.124}Zr_{0.876}O_2$.

The generalized vibrational density of state of $Ce_{0.124}Zr_{0.876}O_2$ was calculated from the measured data of the neutron inelastic scattering performed at 17 K. The results are shown in Figure 3. The large broad peak of the vibrational density of state is observed at the energy range around 18 meV. The peak should be attributed to van Hove singularity due to the phonons near the Brillouin zone boundary extended from the acoustic branch, by referring to the lattice dynamics study of stabilized zirconia.[25] The large vibrational density of state around 18 meV is consistent with the results of the heat capacity measurements. This indicates that the excess heat capacity of $Ce_{0.124}Zr_{0.876}O_2$ is attributed to the softening of the lattice vibrations. In the previous studies,[17] we indicated that the softening should be related to the stabilization of high-temperature phases and not to the formation of oxygen defects. The existence of the excess heat capacity of $Ce_{0.124}$-

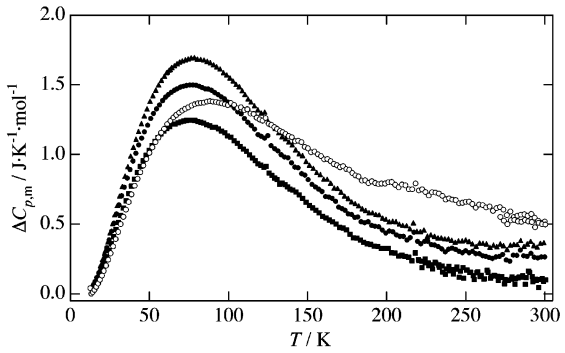

Figure 2. Excess heat capacity of stabilized zirconia: the heat capacity difference $\triangle C_{p,m} = C_{p,m} - C_{p,m}(calc)$. $C_{p,m}(calc)$ was calculated on the assumption of the additivity rule for ZrO_2 and CeO_2/Y_2O_3.[16,17] ○, $Ce_{0.124}Zr_{0.876}O_2$; ▲, $(Y_2O_3)_{0.0776}(ZrO_2)_{0.9224}$; ●, $(Y_2O_3)_{0.0970}(ZrO_2)_{0.9030}$; ■, $(Y_2O_3)_{0.1135}(ZrO_2)_{0.8865}$.

Table 2. Thermodynamic Functions of $Ce_{0.124}Zr_{0.876}O_2$ at Rounded Temperatures: $C^\circ_{p,m}$ Is the Standard Molar Heat Capacity, $\Delta_0^T H^\circ_m$ Is the Standard Molar Enthalpy, $\Delta_0^T S^\circ_m$ Is the Standard Molar Entropy, and $\Phi^\circ_m = \Delta_0^T S^\circ_m - \Delta_0^T H^\circ_m/T$

T	$C^\circ_{p,m}$	$\Delta_0^T H^\circ_m$	$\Delta_0^T S^\circ_m$	Φ°_m
K	J·K^{-1}·mol^{-1}	K	J·K^{-1}·mol^{-1}	K
15	0.1573	0.475	0.0397	0.00798
20	0.4443	1.905	0.1200	0.02473
30	1.674	11.75	0.5025	0.1108
40	3.686	38.01	1.244	0.2939
50	6.199	87.13	2.330	0.5872
60	8.984	162.9	3.703	0.9885
70	11.90	267.2	5.306	1.488
80	14.86	401.1	7.089	2.075
90	17.83	564.5	9.011	2.738
100	20.76	757.5	11.04	3.466
110	23.61	979.4	13.15	4.250
120	26.37	1229	15.33	5.082
130	29.03	1506	17.54	5.955
140	31.58	1810	19.79	6.863
150	34.02	2138	22.05	7.800
160	36.32	2490	24.32	8.762
170	38.51	2864	26.59	9.744
180	40.57	3259	28.85	10.74
190	42.53	3675	31.10	11.75
200	44.37	4109	33.33	12.78
210	46.11	4562	35.53	13.81
220	47.74	5031	37.72	14.85
230	49.27	5516	39.87	15.89
240	50.69	6016	42.00	16.93
250	52.02	6530	44.10	17.98
260	53.26	7056	46.16	19.02
270	54.43	7595	48.19	20.06
280	55.52	8145	50.19	21.10
290	56.55	8705	52.16	22.14
298.15	57.34	9169	53.74	22.98
300	57.51	9275	54.09	23.17

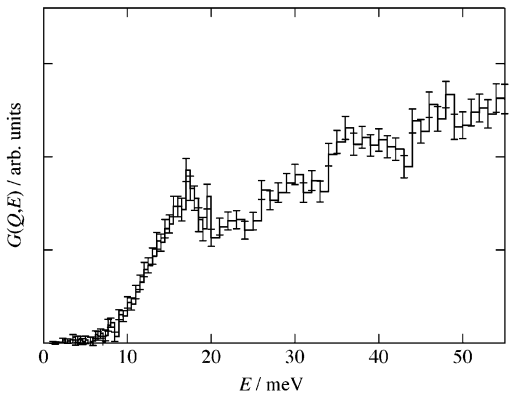

Figure 3. Generalized phonon density of states of $Ce_{0.124}Zr_{0.876}O_2$ calculated from the results of neutron inelastic scattering experiments.

$Zr_{0.876}O_2$, in which no oxygen defects are present in the crystal, excludes the possible effects of the formation of oxygen defects. Therefore, the present study confirms that the stabilization of high-temperature phases does indeed soften the lattice vibrations in stabilized zirconia. In the previous studies,[16,17] we have found the softening caused by yttria-doping, but we could not attribute the mechanism to either the stabilization of the high-temperature phase or the formation of oxygen defects. However, the existence of a similar excess heat capacity in $Ce_{0.124}Zr_{0.876}O_2$, which has no oxygen defects, excludes the possible effects of the formation of vacancies.

Literature Cited

(1) Smith, D. K.; Cline, C. F. Verification of Existence of Cubic Zirconia at High Temperature. *J. Am. Ceram. Soc.* **1962**, *45*, 249−250.

(2) Teufer, G. The Crystal Structure of Tetragonal ZrO_2. *Acta Crystallogr.* **1962**, *15*, 1187.

(3) Smith, D. K.; Newkirk, H. W. The Crystal Structure of Baddeleyite (monoclinic ZrO_2) and its Relation to the Polymorphism of ZrO_2. *Acta Crystallogr.* **1965**, *18*, 983−991.

(4) Etsell, T. H.; Flengas, S. N. The Electrical Properties of Solid Oxide Electrolytes *Chem. Rev.* **1970**, *70*, 339−376.

(5) Aldebert, P.; Traverse, J.-P. Structure and Ionic Mobility of Zirconia at High Temperature *J. Am. Ceram. Soc.* **1985**, *68*, 34−40.

(6) Casselton, R. E. W. Low Field DC Conduction in Yttria-Stabilized Zirconia. *Phys. Status Solidi* **1970**, *(a) 2*, 571−585.

(7) Schmalzried, H. On Correlation Effects of Vacancies in Ionic Crystal. *Z. Phys. Chem. Neue Folge* **1977**, *105*, 47−62.

(8) Allpress, J. G.; Rossell, H. J. Microdomain Description of Defective Fluorite-type Phases $Ca_xM_{1-x}O_{2-x}$ (M=zirconium, hafnium, x=0.1−1.2). *J. Solid State Chem.* **1975**, *15*, 68−78.

(9) Morinaga, M.; Cohen, J. B.; Faber, J., Jr. X-ray Diffraction Study of $Zr(Ca, Y)O_{2-x}$. II. Local Ionic Arrangements. *Acta Crystallogr.* **1980**, *A36*, 520−530.

(10) McClellan, K. J.; Xiao, S.-Q.; Lagerlof, K. P. D.; Heuer, A. H. Determination of the Structure of the Cubic Phase in High-ZrO_2 Y_2O_3−ZrO_2 Alloys by Convergent-beam Electron Diffraction. *Philos. Mag. A* **1994**, *70*, 185−192.

(11) Steele, D.; Fender, B. E. F. The structure of cubic ZrO_2: $YO_{1.5}$ Solid Solutions by Neutron Scattering. *J. Phys. C: Solid State Phys.* **1974**, *7*, 1−11.

(12) Dexpert-Ghys, J.; Faucher, M.; Caro, P. Site Selective Spectroscopy and Structural Analysis of Yttria-Doped Zirconia. *J. Solid State Chem.* **1984**, *54*, 179−192.

(13) Catlow, C. R. A.; Chadwick, A. V.; Greaves, G. N.; Moroney, L. M. EXAFS Study of Yttria-Stabilized Zirconia. *J. Am. Ceram. Soc.* **1986**, *69*, 272−277.

(14) Li, P.; Chen, I.-W.; Penner-Hahn, J. E. X-ray-absorption Studies of Zirconia Polymorphs. II. Effect of Y_2O_3 Dopant on ZrO_2 Structure. *Phys. Rev. B* **1993**, *48*, 10074−10081.

(15) Tojo, T.; Atake, T.; Shirakami, T.; Mori, T.; Yamamura, H. Low Temperature Heat Capacity of Powder and Sintered Samples Yttria-doped Zirconia. *Solid State Ionics* **1996**, *86−88*, 89−92.

(16) Tojo, T.; Atake, T.; Mori, T.; Yamamura, H. Heat Capacity and Thermodynamics Functions of Zirconia and Yttria-stabilized Zirconia. *J. Chem. Thermodyn.* **1999**, *31*, 831−845.

(17) Tojo, T.; Atake, T.; Mori, T.; Yamamura, H. Excess Heat Capacity in Yttria-stabilized Zirconia. *J. Therm. Anal. Calorim.* **1999**, *57*, 447−458.

(18) Tojo, T.; Kawaji, H.; Atake, T. Molecular Dynamics Study on Lattice Vibration and Heat Capacity of Yttria-stabilized Zirconia. *Solid State Ionics* **1999**, *118*, 349−353.

(19) Heuer, A. H.; Chaim, R.; Lanteri, V. The Displacive Cubic→Tetragonal Transformation in Zironia Alloys. *Acta Metall.* **1987**, *35*, 661−66.

(20) Yashima, M.; Hirose, T.; Katano, S.; Suzuki, Y.; Kakihana, M.; Yoshimura, M. Structural Changes of ZrO_2−CeO_2 Solid Solutions around the Monoclinic-Tetragonal Phase Boundary. *Phys. Rev. B* **1995**, *51*, 8018−8025.

(21) Atake, T.; Kawaji, H.; Hamano, A.; Saito, Y. Construction of Adiabatic Calorimeter for Heat Capacity Measurement from Liquid Helium Temperature to 330 K. *Rep. Res. Lab. Eng. Mater., Tokyo Inst. Technol.* **1990**, *15*, 13−23.

(22) Tanaka, T.; Atake, T.; Nakayama, H.; Eguchi, T.; Saito, K.; Ikemoto, I. Heat Capacity and an Incommensurate Phase Transition of Crystalline Bis(4-chlorophenyl)sulfone. *J. Chem. Thermodyn.* **1994**, *26*, 1231−1239.

(23) Inoue, K.; Kanaya, T.; Kiyanagi, Y.; Shibata, K.; Kaji, K.; Ikeda, S.; Iwasa, H.; Izumi, Y. A Crystal Analyzer Type Inelastic Spectrometer Using the Pulsed Thermal Neutron Source. *Nucl. Instrum. Methods Phys. Res., Sect. A* **1993**, *327*, 433−451.

(24) Westrum, E. F., Jr.; Beale, A. F., Jr. Heat Capacities and Chemical Thermodynamics of Cerium(III) Fluoride and of Cerium(IV) Oxide from 5 to 300° K. *J. Phys. Chem.* **1961**, *65*, 353−355.

(25) Liu, D. W.; Perry, C. H.; Feinberg, A. A.; Currat, R. Neutron-scattering Studies of Phonons in Disordered Cubic Zirconia at Elevated Temperatures. *Phys. Rev. B* **1987**, *36*, 9212−9218.

Received for review March 13, 2003. Accepted September 3, 2003.

JE034052Q